JOURNAL OF MATERIALS SCIENCE 40 (2005) 1367–1370

Study of hydrogenated nanoamorphous silicon(na-Si:H) thin film prepared by RF magnetron sputtering for graded optical band gap (E_g^{opt})

HUACONG YU*, RONGQIANG CUI
Institute of Solar Energy, Shanghai Jiaotong University, Shanghai 200240, People's Republic of China
E-mail: yuhuacong@sjtu.edu.cn

HE WANG, HONG YANG
Institute of Solar Energy, Xi'an Jiaotong University, Xi'an 710049, People's Republic of China

BAICHUAN ZHAO, ZHANXIA ZHAO, DUNYI TANG, SHUQUAN LIN, FANYING MENG
Institute of Solar Energy, Shanghai Jiaotong University, Shanghai 200240, People's Republic of China

The schematic of the energy band gap figure of the graded optical band gap (E_g^{opt}) in p-i-n layer in na-Si:H solar cells was given in the paper. The intrinsic hydrogenated nanoamorphous silicon(na-Si:H) thin films with the graded band gap as a function of depth through the films were prepared by varying the processing power, gas pressure, gas composition, and etc., We have carried out a investigation of the relationships between the E_g^{opt} with the crystallization ratio (Xc) and the E_g^{opt} with the nanocrystalline grain size (D) in na-Si:H thin films grown by PECVD on glass substrates through XRD, Raman scattering, transmission. The E_g^{opt} increase with the decreases of the crystallization ratio (Xc) and the nanocrystalline grain size (D).The hydrogen dilution ratio is found to increase basically both the crystallization ratio (Xc) and the nanocrystalline grain size (D). Two relationships in na-Si:H are discussed by the etching effect of atomic hydrogen in the framework of the growth mechanism and the quantum size effect (QSE).
© *2005 Springer Science + Business Media, Inc.*

1. Introduction

Since the photovoltaic properties of na-Si:H thin films is superior than those of a common wide band gap alloy films(a-Si:H). Moreover electronic properties of these films are superior than common a-Si:H thin films under illumination. In recent years, the hydrogenated nanoamorphous silicon(na-Si:H) thin films have attracted considerable interest due to their distinct advantage in solar cells [1–9]. The na-Si:H thin film is a two-phase mixed material, in which nanocrystals embedded in the amorphous silicon tissues in the interface regions among the grains [1, 4–7, 10–12]. Several deposition techniques have been established to prepare na-Si:H thin films, including plasma enhanced chemical vapor deposition (PECVD), radiofrequency (RF) magnetron sputtering, and hot wire chemical vapor deposition (HWCVD) [1–7, 10, 11]. In 1986, the graded optical band gap of solar cells was designed utilized doped C and Ge by Guha et al. [13]. But the doped *C* or Ge will bring some deleterious doped effect in silicon film. In this paper, the graded optical band gap intrinsic na-Si:H was designed utilized the relationships between E_g^{opt} with the crystallization ratio (Xc) and E_g^{opt} with the nanocrystalline grain size (D). Two relationships was also derived by experiment varying the processing power, gas pressure, gas composition, and etc., The X-ray diffraction (XRD) and Raman scattering measurements reveal that the samples are nanocrystalline silicon. Their crystallization ratio (Xc) was obtained from the Raman spectra. Their average grain sizes [$d_{(111)}, d_{(220)}$] were calculated from the width of the (1 1 1) and (2 2 0) diffraction peaks by the Scherrer formula. Their Transmission Electron Micrographs (TEM) gave evidence for the presence of scattered nanocrystallites of <10 nm average size

*Author to whom all correspondence should be addressed.

embedded in the hydrogenated amorphous silicon matrix [8, 9].

2. Experimental procedure and methods

The na-Si:H thin films were prepared in the ultrahigh vacuum (10^{-6} Torr) radio-frequency magnetron sputtering system using process gases silane and hydrogen. Chamber pressure, r.f. power density and substrate temperature range were 60 W and 250–280°C respectively.

We use JG-PF3B three targets radio frequency sputtering equipment to sputter and deposit. Making two corrosion resistant plate as anticathode and cathode, then we place the sputtering single crystal silicon material at cathode and place anticathode, using water-cooling, at underlay; we fill the space between two electrodes with Ar and H_2 and applied electric pressure range is from 0.3 to 1.5 kV. The gas ion forms owning to glow discharge between two electrodes, then the gas ion attacks single crystal silicon surface at cathode with the effect of electric field, this makes Si atoms evaporate from the surface, which become ultramicron and deposit on the surface of underlay. The size and distribution of particles depend on electric pressure, electric current, gas dilution and gas pressure between two electrodes.

Main parameters of this equipment are following:

1.	Degree of vacuum	10^{-5} mmHg
2.	Working electric current	10 A
3.	Shield electric current	0.5 A
4.	Coupling electric current	3 A
5.	High electric voltage	800 V
6.	Gate current	250 mA
7.	Radio frequency frequency	13.56 MHz
8.	Vacuum-chamber diameter	395 mm
9.	The target diameter	80 mm
10.	Maximum sputtering distance	33 mm

The underlay, chosen to use polishing silicon wafer and glass sheet, is placed to Vacuum-chamber after convention cleaning and drying. Before sputtering we use Ar hydroniums to attack in order to wipe off pollutant and gas molecules, this can increase activity of underlay surface and improve binding force between underlay and film.

Experiment basis process flow is as follow Fig. 1. The sputtering discharge power and time, sputtering offset electric pressure, air pressure, the percentage composition of H_2 and Ar are the main parameters of preparation, and change of parameters can effect the microstructure and photoelectricity characteristic of nanoamorphous silicon films.

All the thin films with a layer thickness of around 0.5 μm were deposited on about 1 mm-thick glass substrates at a temperature of 250 to 280°C. The size of average grain sizes of na-Si:H film can be achieved by change the H_2 dilution ratio, The varying of crystallization ratio (Xc) can be obtained by change the high electric voltage between two electrodes, when the the high electric voltage between two electrodes was varied from 1500 to 1800 V, the crystallization ratio (Xc) was 4.21 to 60.76%. The higher of the high electric voltage between two electrodes, the more of the crystallization ratio (Xc) .When the hydrogen dilution ratio R was varied from 33.6 to 156.5, the size of average grain sizes of na-Si:H film was from 9.2 to 2.34 nm; the more of the percentage composition of $H_{2,}$ the smaller of the size of average grain sizes of na-Si:H film [9].

3. Test and analysis

It is very important that accurate determination of the optical constants (refractive index, absorption coefficient and optical band gap) of semiconductor thin-film in solar cell. Mainly two methods for optical characterization were used, i.e., spectroscopic ellipsometry (SE) measurements and the well-known envelope method using the transmission spectrum [14] (or reflection spectrum or both). It is difficult to find an appropriate model for fitting the SE. In contrast to SE, the envelope method has shown relatively higher simplicity and directness as a useful and nondestructive tool for determining the optical constants and thickness of semiconductor thin films deposited on glass substrate. The envelope method based on the ideas of Manifacier *et al.* [15] By using the maxima and minima of the transmission spectrum, was extended by Swanepoel [14], assuming that the glass substrate is transparent and nonabsorbing. However, the actual glass substrates show obvious losses in the optical spectral region [16]. Considering the absorption of the substrate, the transmission $T(\lambda)$ of a system with a four-layer medium configuration. The relatively reasonable optical band gaps can be derived from the original transmission spectra independently by the following equations:

$$T = W \exp(-\alpha d) \tag{1}$$

and

$$\alpha = \frac{B_a}{hv}(hv - E_g)^{\gamma}, \tag{2}$$

where parameter W is found to be nearly unity at the absorption edge [17], E_g^{opt} is the optical band gap, Ba and γ are constants. In the one electron approximation, $\gamma = 1/2$ for allowed direct transitions and 3/2 for forbidden direct transitions. For indirect transition, $\gamma = 2$ [18]. It is well known that nanocrystalline silicon has indirect band structure [18, 19], so we use Tauc plot ($\gamma = 2$) to determine the optical gaps of

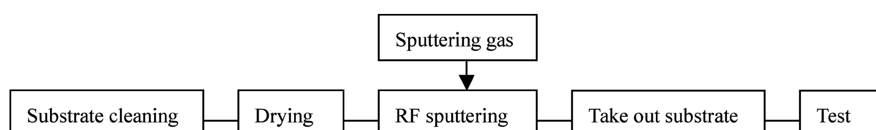

Figure 1 RF sputtering process flow.

TABLE I The relationship between the E_g^{opt} with the crystallization ratio (Xc)

Samples no.	H109	H110	H113	H112	H111	H108	H117	H116	H118	H413	H119	H122	H121
Xc (%)	4.21	12.23	21.12	22.63	29.31	34.31	36.29	38.66	40.6	42.78	46.35	50.55	60.76
E_g^{opt} (ev)	2.11	1.98	1.96	1.95	1.94	1.88	2.13	1.85	1.8	1.79	1.78	1.68	1.6

na-Si:H. Combining Equation 1 (setting $W = 1$) with Equation 2, we have the following relationship:

$$\left(\frac{-h\nu \ln T}{d}\right)^{1/2} \propto (h\nu - E_g) \qquad (3)$$

For na-Si:H, since d is a constant independent of the determination of E_g^{opt}; we simply set all $d = 1$ mm for the all na-Si:H thin films to extrapolate E_g^{opt} in strong absorption regions. The linearity of simulation also confirms the indirect band nature of na-Si:H, rather than the direct one. The corresponding results are presented in Tablse I and II [20].

The X-ray diffraction (XRD) and Raman scattering measurements reveal that the samples are nanocrystalline silicon. Their average grain sizes [$d_{(111)}$, $d_{(220)}$] were calculated from the width of the (1 1 1) and (2 2 0) diffraction peaks by the Scherrer formula, respectively (see Table I). The crystallization ratio (Xc) in Table I was obtained from the Raman spectra. The transmission spectra were performed on a Nicolet Nexus 870 Fourier transform infrared (FTIR) spectrometer from 4000 to 25,000 cm^{-1} (i.e., photon energy from 0.5 to 3.1 eV), avoiding the direct transition of crystalline silicon when the photon energy is up to 3.4 eV [16]. All the measurements were carried out at room temperature.

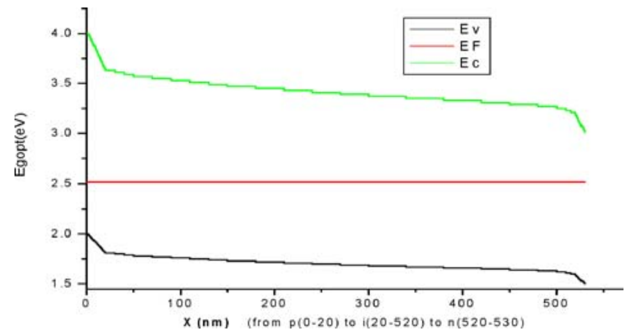

Figure 2 The schematic of the graded varying optical band gap figure of in p-i-n na-Si:H solar cells.

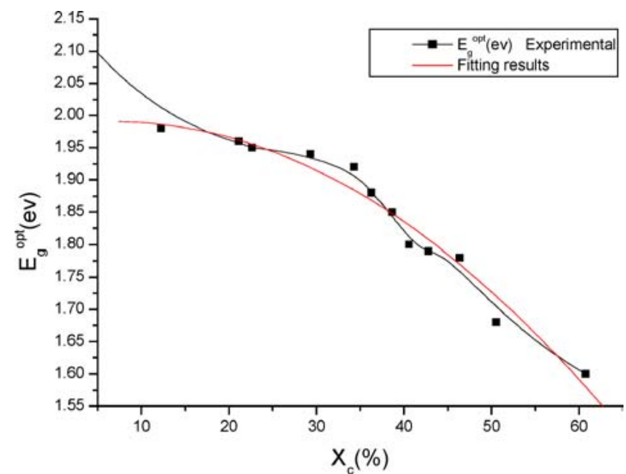

Figure 3 The relationship between the E_g^{opt} with the crystallization ratio (Xc).

4. Results and discussion

Fig. 2 show the schematic of the graded varying optical band gap figure of in p-i-n na-Si:H solar cells.

Such modeling will provide insight into which structures which can be achieved by variations of the process condition.

Table I and Fig. 3 show the relationship between the E_g^{opt} with the crystallization ratio (Xc); Table II and Fig. 4 show the relationship between the E_g^{opt} with the crystallization ratio (Xc).

It is distinct from the two figures that the optical performance for the na-Si:H is different from that of the normal a-Si:H. The hydrogen dilution play an important role in the transition from amorphous to microcrystalline or nanocrystalline phase. It is clear that crystallization ratio (Xc) and the nanocrystalline grain size (D) increase with hydrogen dilution ratio [9]. According the 'selective etching' effect of atomic hydrogen, by plasma increases with the hydrogen dilution ratio, will tend to eliminate the dangling bonds and weak Si—Si bonds to form a rigid and strong Si–Si bond [20], the arriving rate of SiHx to the growth surface increases and the surface diffusion length of SiHx radicals becomes large, which are favorable to form regular Si–Si bonds. Therefore, with increasing hydrogen dilution ratio, the grain size (D) and the crystallization ratio (Xc) of na-Si:H can be enhanced [21]. It is explained that the atomic hydrogen can remove the dangling bonds (i.e., the etching effect) so that the optical band gap increases as a result of the decrease of disorder in the lattice or narrowing of the band tail [22, 23]. Another explaining is that the quantum size effect (QSE) is evident since

TABLE II The relationship between the E_g^{opt} with the nanocrystalline grain size (D)

Samples no.	H003	H004	H006	H007	H010	H008	H017	H011	H016	H015	H019	H022	H023	H026	H027	H028	H030
D (nm)	2.34	2.38	2.42	2.52	2.58	2.62	2.71	2.92	3.06	3.31	3.6	4.3	5.45	6.3	7.2	8.6	9.2
E_g^{opt} (ev)	2.5	2.46	2.42	2.37	2.32	2.28	2.13	2.1	2.06	1.98	1.93	1.9	1.88	1.85	1.81	1.8	1.79

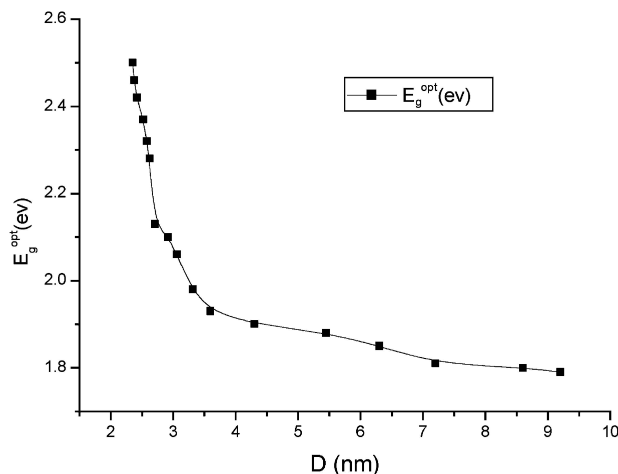

Figure 4 The relationship between the E_g^{opt} with the nanocrystalline grain size (D).

the average grain sizes of the na-Si:H thin films from the XRD measurement are 2.5–10 nm (see Table II). The QSE in na-Si:H have affected the optical band gap [9]. Therefore, the E_g^{opt} increase with the decreases of the crystallization ratio (Xc) and the nanocrystalline grain size (D).

5. Conclusions

The schematic of the energy band gap figure of the graded optical band gap (E_g^{opt}) in p-i-n layer in na-Si:H solar cells was given in the paper. The intrinsic hydrogenated nanoamorphous silicon(na-Si:H) thin films with the graded band gap as a function of depth through the films were prepared by varying the processing parameters. The hydrogen dilution play an important role in the na-Si:H. The optical band gaps derived from Tauc plot increase with decreases of the hydrogen dilution ratio. We have carried out a investigation of the relationships between the E_g^{opt} with the crystallization ratio (Xc) and the E_g^{opt} with the nanocrystalline grain size (D) in na-Si:H thin films grown by RF magnetron sputtering on glass substrates through XRD, Raman scattering, transmission. The E_g^{opt} increase with the decreases of the crystallization ratio (Xc) and the nanocrystalline grain size (D). Two relationships in na-Si:H are discussed by the etching effect of atomic hydrogen in the framework of the growth mechanism and the quantum size effect (QSE), which can successfully explain the experimental results in this work and some other reported results in the literature. Since the graded optical band gap of the na-Si:H could be prepared by RF magnetron sputtering, it can be used as intrinsic layer of the p-i-n solar cell with a graded optical band gap profile. All work established the foundation for carrying out the solar cells with graded optical band gap next step.

Acknowledgements

This work was supported by the Nanometre Science and Technology Project of Shanghai under Contract No. 0216nm103. The authors acknowledge X. Y. Chen and H. Chen at Laboratory of Condensed Matter Spectroscopy and Opto-Electronic Physics, Department of Physics, Shanghai Jiaotong University who tested some samples and thanks for their helpful discussions.

References

1. SUKTI HAZRA, *Solid State Communi.* **109** (1999) 125.
2. SUKTI HAZRA and SWATI RAY, *Jpn. J. Appl. Phys.* **38** (1999) L495.
3. A. V. SHAH, J. MEIER, E. VALLAT-SAUVAIN, N. WYRSCH, U. KROLL, C. DROZ and U. GRAF, *Solar Energy Mater. Solar Cells* **78** (2003) 469.
4. S. HAMMA, P. ROCA and I. CABARROCAS, *ibid.* **69** (2001) 217.
5. TOSHIAKI SASAKI, SHINJI FUJIKAKE and KATSUYA TABUCHI, *et al.*, *J. Non-Cryst. Solids* **266–269** (2000) 171.
6. X. N. LIU and Y. L. HE, *Phy. Rev.* **42**(12) (1993) 1979.
7. Z. H. HU, X. B. LIAO and X. B. ZENG, *et al.*, Optical Characterization of Hydrogenated Amorphous Silicon Carbide Films From Transmission Spectra (to be published).
8. YU HUACONG, CUI RONGQIANG,YANG HONG and WANG HE, *et al.*, *Solar Energy Mater. Solar Cells*, to be published.
9. YU HUACONG, CUI RONGQIANG, YANG HONG and WANG HE, *et al.*, "The 21st Century's New Technology of Solar Energy" (Shanghai Jiaotong University Press, Chinese, 2003) p. 171.
10. J. MEIER, S. DUBAIL, J. CUPERUS, U. KROLL, R. PLATZ, P. TORRES, J.A.A. SELVAN, P. PERNET, N. BECK, N.P.VAUCHER, C. HOF, D. FISCHER, H. KEPPNER and A. SHAH, *ibid.* **227–230** (1998) 1250.
11. J. MEIER, H. KEPPNER, S. DUBAIL, U. KROLL, P. TORRES, P. PERNET, Y. ZIEGLER, J. A. A. SELVAN, J. CUPERUS, D. FISCHER and A. SHAH, *Proc. Mater. Res. Soc. Symp.* **507** (1998) 139.
12. A. ACHIQ, R. RIZK, R. MADELON, F. GOURBILLEAU and P. VOIVENEL, *The Solid Films* **296** (1997) 15; TAWADA, M. KONDO, H. OKAMOTO, *et al.*, *Jpn. J. Appl. Phys.* **21** (Suppl. 21-1) (1982) 297.
13. S. GUHA, J. YANG, P. NATH and M. HACK, *Appl. Phy. Lett.* **49** (1986) 218.
14. R. SWANEPOEL, *J. Phys.* E **16** (1983) 1214.
15. J. C. MANIFACIER, J. GASIOT and J. P. FILLARD, *J. Phys.* **E9** (1976) 1002.
16. J. D. KLEIN, A. YEN and S. F. COGAN, *J. Appl. Phys.* **68** (1990) 1825.
17. Y. DU, M. S. ZHANG, J. WU, L. KANG, S. YANG, P. WU and Z. YIN, *Appl. Phys.* A **76** (2003) 1105.
18. A. NAKAJIMA, Y. SUGITA, K. KAWAMURA, H. TOMITA and N. YOKOYAMA, *J. Appl. Phys.* **80** (1996) 4006.
19. Z. X. MA, X. B. LIAO, G. L. KONG and J. H. CHU, *Appl. Phys. Lett.* **75** (1999) 1857.
20. H. CHEN, M. H. GULLANAR and W. Z. SHEN, *J. Cryst. Growth* **260** (2004) 91.
21. R. MARTINS, I. FERREIRA, F. FERNANDES and E. FORTUNATO, *J. Non-Cryst. Solids* **227–330** (1998) 901.
22. R. PLATZ, S. WAGNER, C. HOF, A. SHAH, S. WIEDER and B. RECH, *J. Appl. Phys.* **84** (1998) 3949.
23. M. YAMAGUCHI and K. MORIGAKI, *Philos. Mag.* **B79** (1999) 387.